

## Short Paper

---

# Morphological De-ringing Filter Design for JPEG-2000

SHEN-CHUAN TAI, CHUEN-CHING WANG, LING-SHIOU HUANG  
AND YING-RU CHEN

*Institute of Electrical Engineering  
National Cheng Kung University  
Tainan, 701 Taiwan*

JPEG2000 plays an important role in image data compression. However, JPEG-2000 produces noticeable image degradation, so-called “ringing artifacts,” in the vicinities of edges in reconstructed images, especially when the images are highly compressed. Ringing artifacts result in artificial contours, thus so degrading the quality of decoded images. To improve the visual quality of decoded images and make them perceptually acceptable, post-processing to accomplish de-ringing is often used. In this paper, an adaptive directional morphological filter (ADMF) to reduce ringing artifacts is presented. Compared with the previously proposed methods, ADMF is rather efficient and effective. Simulation results show that ADMF is capable of significantly reducing ringing artifacts.

**Keywords:** JPEG2000, de-ringing filter, morphological filter, wavelet-based coding, ringing artifacts

## 1. INTRODUCTION

JPEG2000 [1] can encode images at very low bit rates with acceptable quality because, as a wavelet-based coder, it only needs to use a very small portion of the transform coefficients and/or can very coarsely quantize the transform coefficients to achieve acceptable reconstruction. Wavelet-based coders have this property because wavelets form an unconditional basis in a wide range of smooth spaces. However, lossy full-frame wavelet-based image compression generally causes some ringing artifacts, not “sharp” or “peaky” artifacts, around the edges in compressed images. Fig. 1 (a) and Fig. 1 (b) show the original image and the corresponding image reconstructed using wavelet-based coding at 0.07825 bpp, respectively. As can be seen in Fig. 1 (b), at a low bit rate, the ringing artifacts are quite prominent. These artifacts occur regardless of the filter bank chosen and are usually due to the fact that the high frequency components of an image, which play an important role in smoothing “ripple” waveforms, are omitted and/or coarsely quantized in wavelet-based coders. To achieve a low bit rate, however, approximating the highpass coefficients is inevitable.

---

Received October 19, 2001; revised April 10 & June 24, 2002; accepted August 14, 2002.  
Communicated by Kuo-Chin Fan.

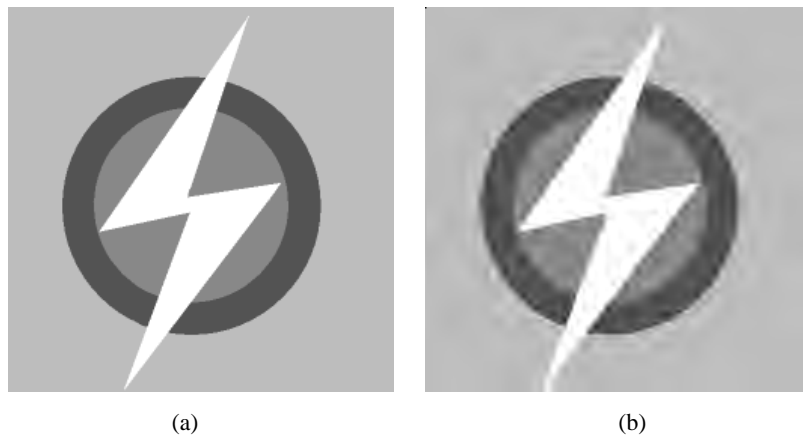


Fig. 1. An example showing how badly the ringing artifacts of a wavelet-based-coded image can degrade the visual quality: (a) original image Flash, (b) JPEG2000-coded Flash at 0.07825 bpp.

In image restoration, the ultimate goal is to build a replica that is as close as possible to the original image. The purpose of “removing ringing artifacts” is to make the smooth regions as smooth as they were in the original image. It should not, however, falsely consider edges as part of ringing artifacts and smooth them. That is, ringing artifacts are removed to make the image more perceptually acceptable.

The paper is organized as follows. In section 2, previous research results on de-ringing are briefly reviewed and discussed. Section 3 discusses general considerations involved in designing morphological de-ringing filters and gives a detailed description of the proposed morphological de-ringing filter. Section 4 compares the new algorithm with previous algorithms. This section also gives examples to show how the algorithm is used to remove ringing artifacts from a low bit rate compressed image. Section 5 concludes the paper.

## 2. PREVIOUS RESEARCH RESULTS

Various de-ringing algorithms, like those in [2-6], have recently been proposed. Since large ringing artifacts are visible and will be mistaken as small features, they all have frequency components as features and are, therefore, not separable in the frequency domain. Hence, linear filters can seldom remove ringing artifacts without destroying the features simultaneously. Linear filters tend either to amplify the noise along the features or smooth out the ringing artifacts and undesirably blur the features at the same time. Linear filters always degrade edges, including boundaries and lines. In particular, they always blur edges. For example, median filters are very good at removing ringing artifacts from smooth areas, but they degrade thin lines and small edges. That is, median filters succeed in removing ringing artifacts but produce unacceptable blurred images.

In [3], Aase and Ramstad proposed heuristics to extract information about shaded regions in an image. With this information, the subband decoder can reduce ringing artifacts by using lowpass projection operators. However, the computation load is heavy and

worse, the heuristics are an inseparable part of the coder. Therefore, their proposed method will not be included in the standard for JPEG 2000.

In a recent article [4], Yang and Galatsanos presented an iterative image restoration method, which is based on projection onto convex sets (POCS), to remove blocking and ringing artifacts. It was designed primary for the DCT based coder and therefore, is not suitable as a post-processor for JPEG2000. This is another computationally intensive post-processing approach, which requires the availability of the entire decoded image. It also requires a large storage space to save the whole image since the POCS requires that the entire image be available.

The de-ringing algorithm proposed by Shen and Kuo [2], which is also described in JPEG2000 VM 5.2 [1], is considered to be suitable as a post-processor for JPEG2000. The de-ringing algorithm replaces each pixel value with a function of the values of the neighboring pixels that are within a specified window. To minimize the conflict between the aforementioned goals, i.e., smoothing shade regions and sharpening at edges, the de-ringing algorithm uses a number of adaptive noise reduction algorithms. Essentially, the de-ringing algorithm attempts to detect edges in the image and handles the regions near the edges in a different way in order to preserve them. Shen and Kuo also formulated the post-processing process as a maximum a posteriori (MAP) estimation and introduced the idea of image ringing artifacts reduction through nonlinear filtering by using different kinds of potential functions. For further details, interested readers may refer to [2].

In this paper, an alternative spatial method, called the morphological filtering scheme [7-10], is proposed to preserve features and remove ringing artifacts. We shall compare our algorithm with Shen and Kuo's algorithm since it performs better than others and is also described in JPEG2000 VM 5.2.

### 3. DESIGNING MORPHOLOGICAL DE-RINGING FILTERS

#### 3.1 1-D Gray-Scale Morphological Filters

The morphological operation was originally designed for set theory. It was then extended and applied to gray-scale images. Readers may refer to [11, 12] for further details. The two basic operations are dilation and erosion, which are described as follows:

$$\text{dilation: } d(f, s)(x) = \max \{f(x+i) \mid i \in D_s\}, \quad (1)$$

$$\text{erosion: } E(f, s)(x) = \min \{f(x+i) \mid i \in D_s\}, \quad (2)$$

where  $f(x)$  is the input signal and  $D_s$  is the domain covered by a structuring element of the  $s$  type. As indicated by (1) and (2), dilation (erosion) takes the maximum (minimum) value within the SE domain.

Combining these two operations leads to two useful operations described as follows:

$$\text{closing: } C(f, s) = E(D(f, s), s), \quad (3)$$

$$\text{opening: } O(f, s) = D(E(f, s), s). \quad (4)$$

Consider the effects of these basic operations on a ringing signal. Fig. 2(a) shows a scan line from Fig. 1(a), and Fig. 2(b) shows the corresponding scan line from Fig. 1(b). Thus, Fig. 2(a) can be considered as an original 1-D waveform, while Fig. 2(b) is a ringing waveform obtained from Fig. 2(a). Fig. 3 shows the simple flat SE. The results of applying the erosion, dilation, opening and closing operations to the ringing waveform of Fig. 2(b), using the flat SE shown in Fig. 3, are illustrated in Fig. 4(a), (b), (c), (d) and (e), respectively. As can be seen from the results, the opening operation smoothes the convex parts within the SE domain, while the closing operation smoothes the concave parts. The results thus suggest application of the opening operation to the convex parts and closing operation to the concave parts. Therefore, we find that averaging that closing and opening results will remove ringing artifacts while preserving the features. From Fig. 4(e), it can be found that the results of averaging the closing and opening results have a better performance in reducing the ringing artifacts.

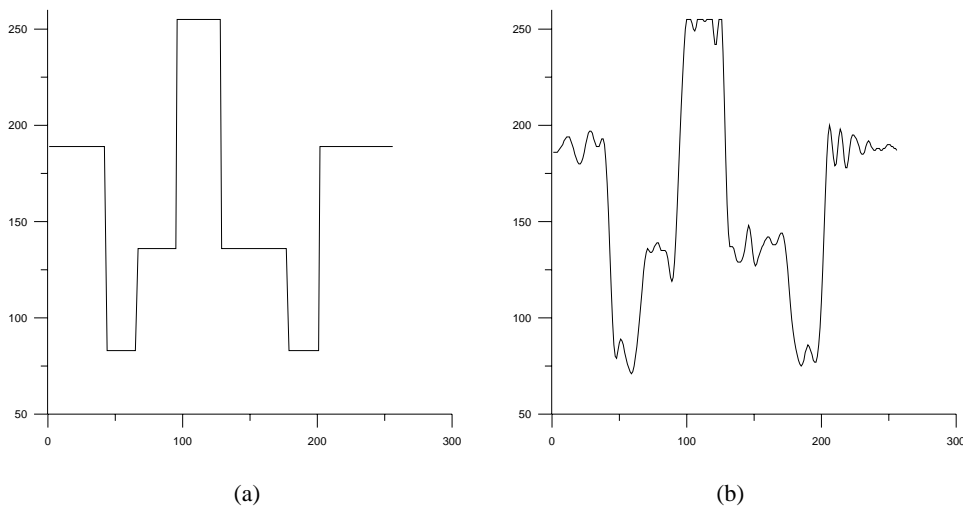


Fig. 2. (a) Original 1-D signal extracted from Fig. 1 (a), (b) ringing signal obtained from the corresponding row of Fig. 1 (b).

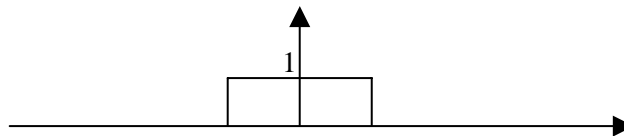


Fig. 3. A flat SE.

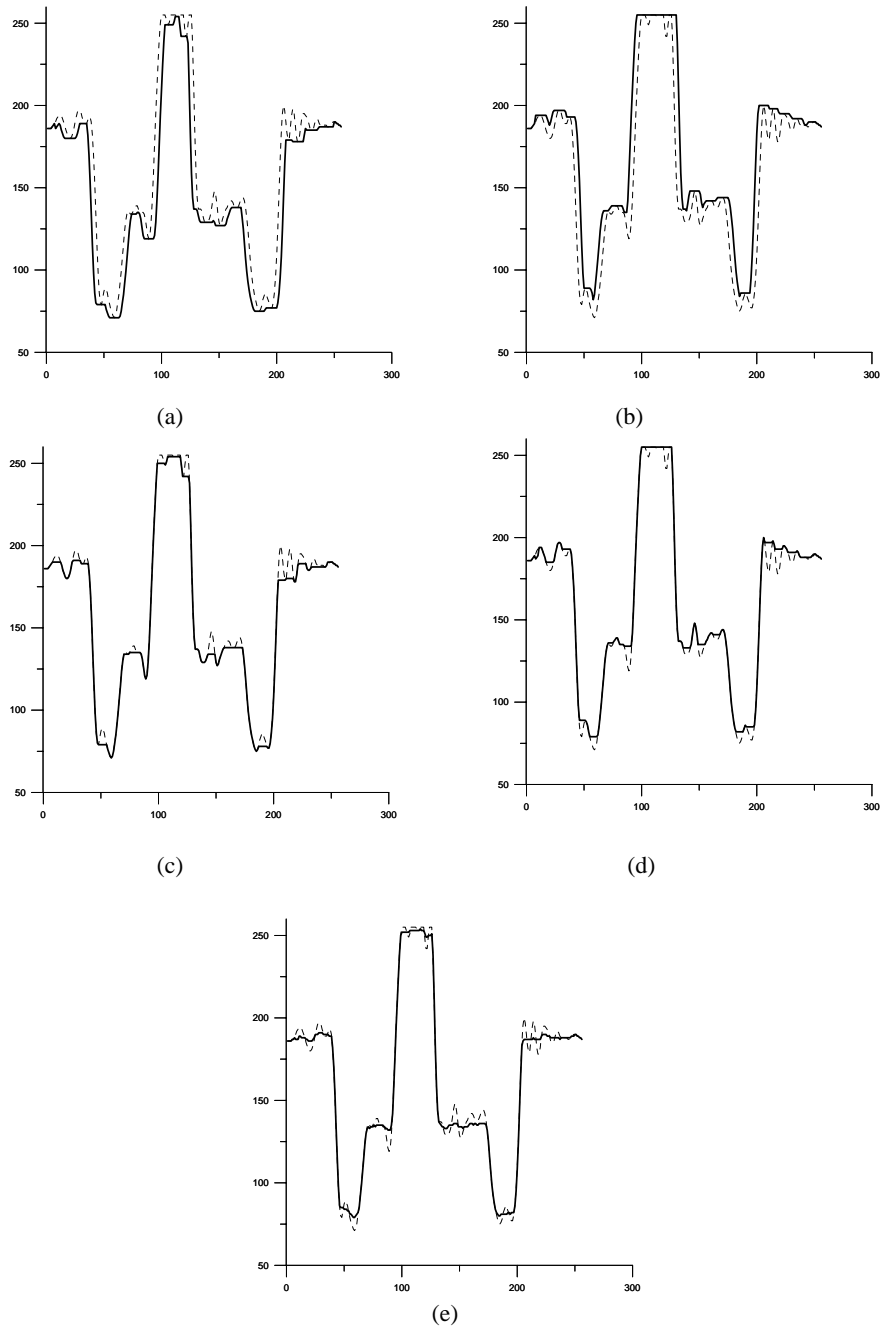


Fig. 4. Morphological filtering performed using various operations, where the dashed line shows the ringing signal and the solid line shows the filtered signal: (a) eroded signal, (b) dilated signal (c) opened signal, and (d) closed signal, and (e) average of the closing and opening results.

### 3.2 Texture Detector

Since ringing artifacts construct new contours, conventional edge detection methods, like the Sobel operator, falsely detect ringing artifacts as edges. Consider the difference between ringing artifacts and image features, including edges and thin lines. An image region is considered by human visual system to contain image features if there exist large transients in it. Thus, determining the presence of edges and other kinds of features depends on the use of a texture detector that can precisely locate large transients. If the threshold is properly selected, the texture detector will be able to distinguish features from ringing artifacts. Hence, variance is used as a classification criterion in the texture detector, which generates a texture map for later reference. In this paper we define the local variance  $\hat{\sigma}^2$  for coordinate  $(u, v)$  as the gray-level variance of the  $3 \times 3$  block centered at  $(u, v)$ . Then, the texture map  $E = \{e(u, v) | e(u, v) \in \{0, 1\}, 0 \leq u, v < N\}$  is generated by the texture detector according as follows:

$$e(u, v) = \begin{cases} 1, & \text{if } \hat{\sigma}^2(u, v) \geq \hat{\sigma}_c^2; & \text{in texture region} \\ 0, & \text{if } \hat{\sigma}^2(u, v) < \hat{\sigma}_c^2; & \text{not in texture region,} \end{cases} \quad (5)$$

where  $\hat{\sigma}_c^2$  is a constant threshold. Thus,  $E$  is a bit map of the same size as the artifact image  $I$ .

Binary dilation is essential in the proposed method. It uses an SE of size 11, i.e.,  $k = 5$ . Consider the case where two edges in a gray-scale image of size  $N \times N$ ,  $I = \{i(u, v) | 0 \leq i(u, v) \leq 255, 0 \leq u, v < N\}$ , are very close to each other. The texture detector will successfully detect the two edges as texture and suggest the use of  $O(I, SE_{n,1})$  and  $C(I, SE_{n,1})$ , instead of  $O(I, SE_{n,5})$  and  $C(I, SE_{n,5})$ . In addition, the texture detector will detect the region between the two edges as a non-texture region and, thus, suggest the use of  $O(I, SE_{n,5})$  and  $C(I, SE_{n,5})$ . Considering (1)-(4), suppose that the size of SE is larger than the width of the region between the two edges; then, the gray-scale of the region bounded by the two edges will "almost" be replaced by that of the background. This will result in appreciable distortion. To solve this problem, we first apply the binary dilation operator to  $E$  and then modify the status of those corresponding bits which belong to the region between the two near edges. At this point,  $E$  has been modified and dilated as the dilated map  $E' = \{e'(u, v) | e'(u, v) \in \{0, 1\}, 0 \leq u, v < N\}$ . Since  $e'(u, v) = 1$  suggests the use of a small SE, which prevents the small region between the two near edges from being destroyed by the large background and, thus, makes the de-ringed image perceptually better.

### 3.3 Directional 1-D SEs

Referring to Fig. 5, the four SEs are identified as  $SE_{1,k}$ ,  $SE_{2,k}$ ,  $SE_{3,k}$ , and  $SE_{4,k}$  for  $k = 2$ , respectively. Each SE corresponds to one direction. Since they are all binary SEs, which contain only 1's and 0's, they are relatively simple to code and implement. Indeed, only a comparator is needed for the morphological operation. When the four SEs are applied in de-ringing, an  $N \times N$  image is regarded as a matrix,  $I$ , and each column, each row, each  $45^\circ$  scan line, and each  $135^\circ$  scan line of the matrix is treated as a 1-D vector.

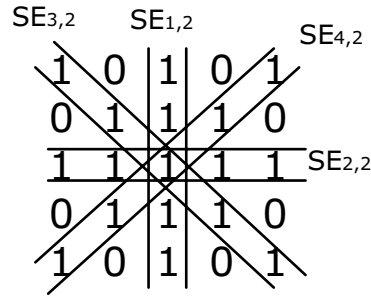


Fig. 5. Four flat structuring elements with different scanning directions of size  $k = 2$ .

Consider the size of SE. It has a direct effect on texture preservation. For example, increasing the size of SE makes the whole image smoother and, therefore, preserves less texture information, in particular, edge information. The size should be as small as possible to just accommodate the maximal widths of the ringing artifacts. In this study, the distributions of ringing artifacts from five  $512 \times 512$ -ringing images were gathered and studied. It was found that by using 11 as the SE size, almost all ringing artifacts could be covered. Referring to Fig. 5, let  $SE_{n,k}$  denote the  $n$ -th SE used, and let it be of size  $2k + 1$ . That is,

$$SE_{1,k}(0, y) = \{ 1 \mid -k \leq y \leq k \}, \quad (6)$$

$$SE_{2,k}(x, 0) = \{ 1 \mid -k \leq x \leq k \}, \quad (7)$$

$$SE_{3,k}(x, y) = \{ 1 \mid x = -y \text{ and } -k \leq x \leq k \}, \quad (8)$$

$$SE_{4,k}(x, y) = \{ 1 \mid x = y \text{ and } -k \leq x \leq k \}. \quad (9)$$

It is clear that  $SE_{1,k}$  is a vertical SE,  $SE_{2,k}$  is a horizontal SE,  $SE_{3,k}$  is a  $135^\circ$  SE, and  $SE_{4,k}$  is a  $45^\circ$  SE. In general,  $k$  can be dynamically adjusted according to the image characteristics.

### 3.4 The Proposed De-ringing Artifact Algorithm

Let the ringing image of size  $N \times N$  be  $I = \{ i(u, v) \mid 0 \leq i(u, v) \leq 255 \}$ , and let the de-ringing filtered image be  $I'$ . As the block diagram of the proposed method shown in Fig. 6 reveals, the process proceeds as follows. First, the texture detector yields a bit map  $E = \{ e(u, v) \mid e(u, v) \in \{ 0, 1 \}, 0 \leq u, v < N \}$  according to the corresponding variance of each pixel in  $I$ . Then, to make the de-ringed image perceptually better, we apply binary dilation in  $E(u, v)$  to generate a dilated version of  $E(u, v)$ , i.e.,  $E'(u, v) = \{ e'(u, v) \mid e'(u, v) \in \{ 0, 1 \}, 0 \leq u, v < N \}$ ; this process prevents the small region between the two near edges from being destroyed by the large background. After that, the operations of ADMF are applied to each pixel in  $I$  using a distinct SE; thus, we finally obtain a de-ringed, filtered image  $I'$ . Briefly, referring to Fig. 6, the proposed method can be summarized as follows.

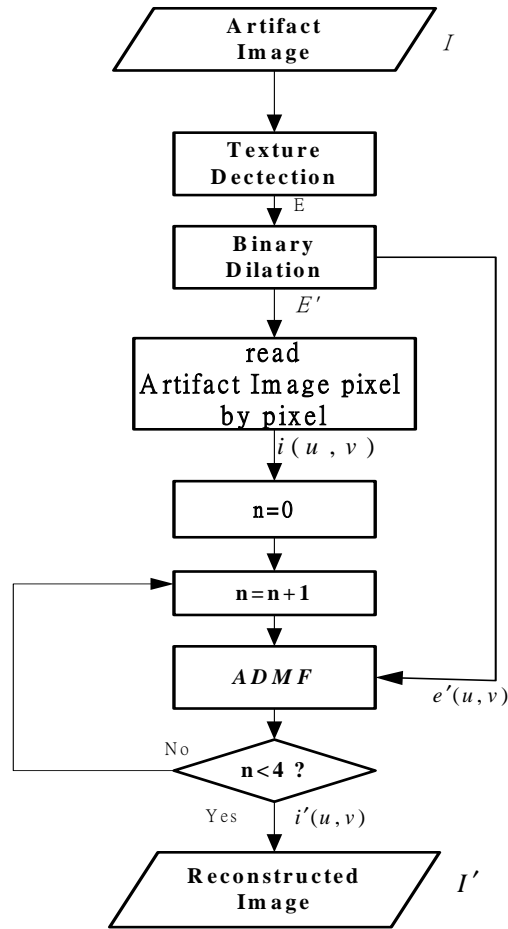


Fig. 6. Block diagram of the proposed algorithm.

**Step 1.** Generate a texture map,  $E = \{e(u, v) \mid e(u, v) \in \{0, 1\}, 0 \leq u, v < N\}$ , from  $I$  using texture detection according to the following rule:

$$e(u, v) = \begin{cases} 1, & \text{if } \hat{\sigma}^2(u, v) \geq \hat{\sigma}_c^2; & \text{in texture region} \\ 0, & \text{if } \hat{\sigma}^2(u, v) < \hat{\sigma}_c^2; & \text{not in texture region,} \end{cases} \quad (10)$$

where  $\hat{\sigma}^2(u, v)$  is the corresponding variance of  $i(u, v)$  generated with a  $3 \times 3$  window and  $\hat{\sigma}_c^2$  is a constant value.

**Step 2.** For  $n = 1$  to 4 and  $k = 5$ , dilate the texture map as dilated version ( $E'$ ) by means of a dilation operation:

$$E' = D(E, SE_{n,k}). \quad (11)$$

**Step 3.** For  $n = 1$  to 4, each pixel  $i(u, v)$  in  $I$  and its corresponding bit  $e'(u, v)$  in  $E'$ , the de-ringed filtered result of each pixel can be expressed as

$$i_n(u, v) = \begin{cases} 1/2[C(I, SE_{n,1})(u, v) + O(I, SE_{n,1})(u, v)] & \text{if } e'(u, v) = 1 \\ 1/2[C(I, SE_{n,5})(u, v) + O(I, SE_{n,5})(u, v)] & \text{if } e'(u, v) = 0, \end{cases} \quad (12)$$

where  $i_n(u, v)$  denotes the de-ringed filtered pixel generated from the pixel  $i(u, v)$  subjected to a morphological operation in the  $n$ -th iteration;  $C(\cdot)(u, v)$  and  $O(\cdot)(u, v)$  denote the closing operation and opening operation applied to each pixel  $i(u, v)$  respectively.

**Step 4.** Output the de-ringed filtered image,  $I' = I_n = \{i_n(u, v) \mid 0 \leq u, v < N\}$ ; here,  $n = 4$ .

In the proposed method, the artifact image is filtered by ADMF in four iterations. In the first iteration, ADMF is processed by using  $n = 1$ ; thus, SE is of the type  $SE_{1,k}$ . Similarly, in the second, third and fourth iteration, the ADMF operation is performed with  $n = 2, 3$  and 4, and SE is of the type  $SE_{2,k}, SE_{3,k}$  and  $SE_{4,k}$ , respectively. In fact, the output of the  $(n-1)$ -th iteration serves as the input of the  $n$ -th iteration. The input of the first iteration is the image to be filtered to achieve de-ringing.

#### 4. RESULTS

In this paper,  $\hat{\sigma}_c^2 = 100$  was used as classification criteria in our experiments. The performance of the proposed morphological filters for ringing artifact reduction is illustrated in this section using two kinds of images (a synthetic image and a natural image) at various bit rates. The ringing artifacts in these images that were compressed using the wavelet codec became more and more prominent as the compression ratio increased. The restoration results were compared with the results reported in [2]. The performance was measured based on

$$PSNR = 10 \log_{10} \frac{255^2}{\frac{1}{N^2} \sum_{i=1}^N \sum_{j=1}^N [p(i, j) - p'(i, j)]^2}, \quad (13)$$

where  $p(i, j)$  and  $p'(i, j)$  are the reference image and reconstructed image, respectively.

The first example is a synthetic image named "lighting" with 256-gray-level luminance, which is shown in Fig. 1 (a). It contains large features and some small features. Fig. 7 (a) shows a ringing image compressed using JPEG2000 at 0.07825 bpp. It contains serious ringing artifacts around the edges. Fig. 7 (b) shows the results obtained using the proposed morphological filtering technique. As can be seen from Fig. 7 (b), most of the ringing artifacts were removed while the edges are well preserved. It is perceptually better than the ringing image shown in Fig. 7 (a). To compare our results with those reported in [2], the parameters in Shen and Kuo's algorithm were defined first. Many sets of parameters were tried, and the set that produced the best results was used. They were  $r = 0.02$  and  $Th = 30$ , and the size of the filtering window was  $w \times w = 25$ . The resulting image produced using this set of parameters is shown in Fig. 7(c). It shows that

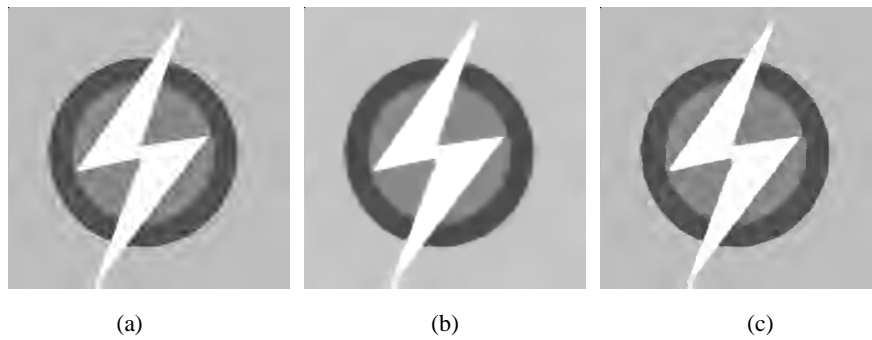


Fig. 7. (a) Decoded image at 0.07825 bpp, (b) de-ringing filtered image after the application of ADMF, and (c) de-ringing filtered image by Shen and Kuo's algorithm.

the quality was improved by Shen and Kuo's algorithm. However, the features were also obliterated. In particular, the regions of the edges are not very smooth, and the smooth regions are fragment-like. In addition, the experimental results show that the objective performance observed in Fig. 7 (c) is poorer than that observed in Fig. 7 (b) by about 0.5 dB. Some examples used for simulation were natural images with 256-gray-level luminance. Figs. 8 (a) and 9(a) show ringing images compressed using the wavelet codec at 0.07935 bpp, 0.05185 bpp and 0.07806 bpp, respectively. Versions of the images restored using the proposed method are shown in Figs. 8(b) and 9(b), respectively. To further compare our results with those reported in [2], which are shown in Figs. 8(c) and 9(c) with parameters  $r = 0.01$  and  $Th = 30$ , and where the size of the filtering window was  $w \times w = 25$ , which achieved the best performance. The results shown in Figs. 8(c) and 9(c) also reveals poor performance around edges and fragment-like phenomena exist in smooth areas.

The PSNRs, including the global, surface and texture PSNRs, of the simulation results at different bit rates for the two test images are summarized in Tables 1 and 2. In general, as the bit rate decreased, the ringing artifacts became more and more prominent. As can be seen from Table 1 and Table 2, the proposed technique achieves better PSNR

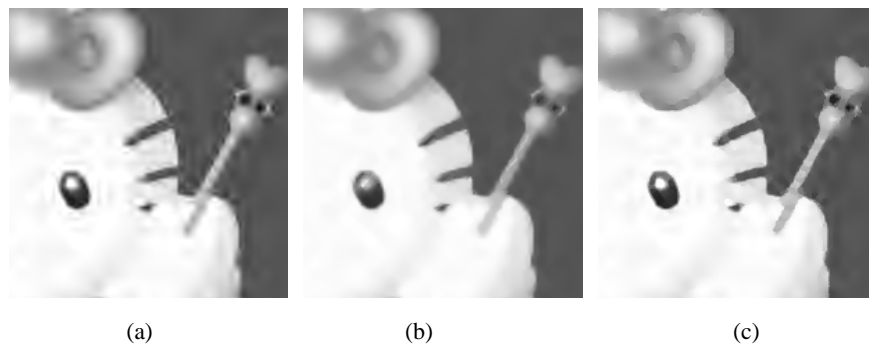


Fig. 8. (a) Decoded image at 0.05185, (b) de-ringing filtered image after the application of ADMF, and (c) de-ringing filtered image by Shen and Kuo's algorithm.

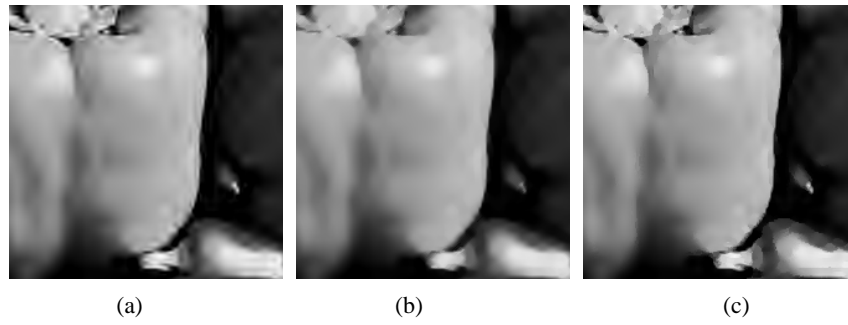


Fig. 9. (a) Decoded image at 0.07806 bpp, (b) de-ringing filtered image after the application of ADMF, and (c) de-ringing filtered image by Shen and Kuo's algorithm.

**Table 1. Comparison of the objective performance of comparison between ADMF and by Shen and Kuo's algorithm. (Compression using JPEG2000 [1]; test image: Lena, parameters:  $r = 0.02$ ,  $Th = 30$  and  $w = 5$ .)**

Bit rate(level =5)	Original PSNR [dB]			Type	PSNR [dB]		
	Global	Surfaces	Textures		Global	Surfaces	Textures
0.1536bpp(52:1)	25.6961	30.2096	21.8668	ADMF	25.4617	30.3417	21.8516
				Ref. [2]	24.9647	30.2569	21.0162
0.1123bpp(71:1)	25.5309	29.8759	21.7122	ADMF	25.3574	30.1866	21.7476
				Ref. [2]	24.9005	29.9425	20.9716
0.09613bpp (83:1)	25.3669	29.4743	21.5871	ADMF	25.1984	30.0613	21.5965
				Ref. [2]	24.8042	29.5822	20.9047
0.07935bpp (100:1)	25.1485	29.0326	21.4066	ADMF	25.0205	29.6015	21.4674
				Ref. [2]	24.6274	29.1198	20.7681
0.06473bpp (123:1)	24.9143	28.4952	21.2298	ADMF	24.8671	29.0069	21.3738
				Ref. [2]	24.4751	28.5916	20.6750
0.05212bpp(154:1)	24.6028	28.0734	21.0113	ADMF	24.6042	28.7979	21.1138
				Ref. [2]	24.2214	28.1654	20.4285

**Table 2. Comparison of the objective performance of ADMF and Shen and Kuo's algorithm. (Compression using JPEG2000 [1]; test image: Flash, parameters:  $r = 0.02$ ,  $Th = 30$  and  $w = 5$ .)**

Bit rate	Original PSNR [dB]			Type	PSNR [dB]		
	Global	Surfaces	Textures		Global	Surfaces	Textures
0.1528bpp (52:1)	28.0510	39.7786	20.7175	ADMF	28.4731	44.3533	20.9854
				Ref. [2]	27.437	41.7212	20.3918
0.1115bpp (71:1)	27.8794	38.6521	20.7353	ADMF	28.3060	43.0395	20.9745
				Ref. [2]	27.6226	40.4684	20.3587
0.09692bpp(82:1)	27.6978	37.2297	20.7164	ADMF	28.1515	41.6814	20.9158
				Ref. [2]	27.515	38.8554	20.3879
0.07825bpp(102:1)	27.3843	36.0828	20.7204	ADMF	27.8624	40.0670	20.9137
				Ref. [2]	27.4465	37.3031	20.66
0.06567bpp(122:1)	26.7967	34.9181	20.3953	ADMF	27.2848	38.3910	20.6903
				Ref. [2]	26.9197	35.8187	20.4195
0.05115bpp(156:1)	26.0763	33.1058	19.8415	ADMF	26.5457	36.0776	20.3667
				Ref. [2]	26.4119	33.7745	20.1172

values compared to those of the original ringing image due to wavelet coding and to those of the de-ringed images using Shen and Kuo's algorithm by about 0.5 ~ 1 dB. In addition, the visual results obtained from the proposed technique are perceptually better than those by Shen and Kuo's algorithm.

We will next consider the computation complexity of the proposed method. Each opening and closing operation is performed using one maximum and one minimum operation. Since a maximum or minimum operation with  $m$  inputs takes  $m-1$  comparison operations, the number of comparison operations required to perform an opening (closing) operation is  $2m-2$ .  $SE_{n,k}$ , which has  $2k + 1$  inputs, thus takes  $2m-2 = 2(2k + 1)-2 = 4k$  comparison operations. Hence, referring to Fig. 6, in each iteration, an ADMF requires 8 ~ 40 comparison operations to implement the morphological opening and closing operation. In the worst case, each iteration per pixel requires including 20 comparison operations for opening by  $SE_{n,5}$  and 20 comparison operations for closing by  $SE_{n,5}$ . On the other hand, in the best case, 4 comparison operations are needed for opening by  $SE_{n,1}$  and 4 are needed for closing by  $SE_{n,1}$ . Two averaging operations need to be performed in the morphological filter, and each averaging operation can be performed using by one add operation and one shift operation. In the worst case, each pixel in ADMF takes four iterations; hence, the total number of comparison operations is 160, and 4 add operations and 4 shift operations are required to compute each pixel in the ADMF procedure. Next, let us consider the operations required for texture detector and binary dilation. Binary dilation can be implemented using an OR gate with 11 inputs. Also, we use an OR gate to decide whether bit  $e'(u, v)$  is equal to 1 or not. As for the texture detector, it takes 25 adders, 9 multipliers, one divider, and one comparator. As compared with [2] and as mentioned above in the discussion, it can be found that ADMF is a low-complexity de-ringing filter.

## 5. CONCLUSIONS

In this paper, a new algorithm for reducing ringing artifacts in a wavelet-based decoded image has been presented. The experimental results show that the visual performance is better than that of previous research results. In addition, the filter is very simple and adapts itself to the image contents by varying the size of the SE. The use of a morphological filter and local adaptation of edges have been shown to be effective for removing ringing artifacts.

As compared with previously proposed de-ringing filters, it is found that the morphological filter approach proposed in this paper has the following advantages:

- (i) It achieves better results both in PSNR and visual perception.
- (ii) It is computationally simpler.
- (iii) It preserves the features well.

However, the proposed algorithm, as is the case with many adaptive methods, requires a number of tuning parameters measured based on the ringing data. It is found that the restoration results are relatively sensitive to the choices of these parameters. Therefore, a subject of the future investigation will be automatic identification procedures for tuning the parameters.

In addition to these parameters, a 1-D morphological filter is used in the proposed algorithm. A disadvantage of the 1-D morphological filter is that it should incorporate four directions. If there are some suitable 2-D structure elements, the proposed algorithm will not have to incorporate iterative processes. Therefore, finding suitable 2-D or other types of structure element is another subject of future investigation.

The morphological de-ringing filter proposed in this paper is quite simple and effective. In fact, most morphological filters are simple and suitable for hardware implementation. We expect that morphological filters will play an important role in de-ringing filter designs and deserve further study.

## REFERENCES

1. "JPEG-2000 verification model 5.2," ISO/IEC JTC 1/SC 29/WG 1 N1422, August 27, 1999.
2. M. Y. Shen and C.-C. Jay Kuo, "Artifact reduction in low bit rate wavelet coding with robust nonlinear filtering," *IEEE Second Workshop on Multimedia Signal Processing*, 1998, pp. 480-485.
3. S. O. Aase and T. A. Ramstad, "Ringing reduction in low bit rate image subband coding using projection onto a space of paraboloids," *Signal Processing: Image Communication*, 1993, pp. 272-283.
4. Y. Yang and N. P. Galatsanos, "Artifact reduction in low bit rate using projections onto convex sets and line process modeling," *IEEE Transactions on Image Processing*, Vol. 6, 1997, pp. 1345-1357.
5. T. P. O'Rourke and R. Stevenson, "Improved image decompression for reduced transform coding artifacts," *IEEE Transactions on Circuits and Systems for Video Technology*, Vol. 5, 1995, pp. 490-499.
6. A. Kaup, "Reduction of ringing noise in transform image coding using simple adaptive filter," *Electronics Letters* 29th, Vol. 34, 1998, pp. 2110-2112.
7. C. R. Giardina and E. R. Dougherty, *Morphological Methods in Image and Signal Processing*, Englewood Cliffs, NJ: Prentice-Hall, 1988.
8. A. C. P. Loui, A. N. Venetsanopoulos, and K. C. Smith, "Flexible architectures for morphological image processing and analysis," *IEEE Transactions on Circuits and Systems for Video Technology*, Vol. 2 1992, pp. 72-83.
9. K. I. Diamantaras, K. H. Zimmermann, and S. Y. Kung, "Integrated fast implementation of mathematical morphology operations in image processing," *IEEE International Symposium on Circuits and Systems*, Vol. 2, 1990, pp. 1442-1445.
10. A. C. P. Loui, A. N. Venetsanopoulos, and K. C. Smith, "High-speed architecture for morphological processing," *Nonlinear Image Processing, SPIE*, Vol. 1247, 1990, pp. 145-156.
11. O. Egger, W. Li, and M. Kunt, "High compression image coding using an adaptive morphological subband decomposition," in *Proceedings of the IEEE*, Vol. 83, 1995, pp. 272-287.
12. R. A. Peters, II, "A new algorithm for image noise reduction using mathematical morphology," *IEEE Transactions on Image Processing*, Vol. 4, 1995, pp. 554-568.

**Shen-Chuan Tai (戴顯權)** received BS and MS degree in electrical engineering from the National Taiwan University, Taipei, in 1982 and 1986, respectively, and a PhD degree in computer science from the National Tsing Hua University, Hsinchu, Taiwan, in 1989. From 1989 to 1997, he was an associate professor of electrical engineering at the National Cheng Kung University, Tainan, Taiwan. He is now a professor at the same institute. Prof. Tai has published more than 110 papers. His teaching and research interests include data compression, multimedia communications, DSP VLSI array processor, computerized electrocardiogram processing, and algorithms.

**Chuen-Ching Wang (王春清)** The author was born in Kaushung, Taiwan, R.O. C., on February 19, 1959. He received BS and MS degree in electrical engineering from the National Cheng Kung University, Taiwan, in 1986 and 1994, respectively. He is currently working toward his PhD at the institute of electrical engineering, National Cheng Kung University. Also, he is now a section chief at Directorate General Telecommunications in Ministry of Transportation and Communications. His research interests include digital signal processing, image processing, DAB receiver chip design and multimedia communications.

**Ling-Shiou Huang (黃鈴秀)** The author was born in Taipei, Taiwan, R.O.C., on May 2, 1975. She received BS degree in National Taipei Institute Technology, Taiwan, in 1995, and received MS degree in electrical engineering from the National Cheng Kung University, Taiwan, in 2000. Her research interests include data compression, digital watermarking, image processing, and multimedia communications.

**Ying-Ru Chen (陳滢如)** was born in Tainan, Taiwan, R.O.C., on September 11, 1976. She received the BS degree of Information Computer and Education from National Taiwan Normal University, Taipei, Taiwan, in 2000, and received MS degree in electrical engineering from the National Cheng Kung University, Taiwan, in 2002. Her research interests include data compression, digital watermarking, information security, and data communication.